Polarization Effects in Collision-Induced Intramultiplet Mixing for $Ne^{**}\{(2p)^5(3p)\}+He$

M. P. I. Manders, J. P. J. Driessen, H. C. W. Beijerinck, and B. J. Verhaar
Physics Department, Eindhoven University of Technology, Eindhoven, The Netherlands
(Received 27 December 1985)

High-quality polarized-emission cross sections for the $\{\alpha\}_5=|J=1,M_J\rangle \rightarrow \{\alpha\}_7$ and $\{\alpha\}_5 \rightarrow \{\alpha\}_4$ transitions in the $\{\alpha\}=\{(2p)^5(3p)\}$ multiplet (lifetime 20 ns) have been measured in a crossed-beam experiment. For the $\{\alpha\}_5 \rightarrow \{\alpha\}_7$ transition we observe a strong preference for the $|M_J|=0$ orientation. The small cross section for the $|M_J|=1$ orientation can be understood qualitatively from the model potentials of Hennecart and Masnou-Seeuws by the strong coupling to the $\{\alpha\}_4$ and $\{\alpha\}_6$ states (avoided crossings), which is absent for the $\Omega=|M_J|=0^-$ molecular potentials because of the constraint of reflection symmetry.

PACS numbers: 31.50.+w, 34.50.Pi, 34.50.Rk

Inelastic collisions of atoms in short-lived, electronically excited states presently are in the focus of attention of both theorists[1-4] and experimentalists.[5-11] A recent review of the field has been given by Hertel.[12] The dependence of the outcome of the collision process on the initial orientation of the electronic angular momentum with respect to the initial relative velocity of the collision partners has proven to reveal many interesting features of the potential surfaces and collision dynamics.[2,6,7] So far, most experiments have been performed in bulk. Only recently have crossed-beam experiments with a much better defined initial relative velocity been reported,[6,7] resulting in more reliable results on these polarization effects. Until now, the rather simple one-electron alkali-metal[4-6,13-15] and two-electron alkaline-earth[3,7-9] systems have received most attention.

In this paper we report the first crossed-beam study of inelastic, fine-structure–changing collisions for the system

$$Ne^{**}[\{(2p)^5(3p)\}_k;J_k]+He \rightarrow Ne^{**}[\{(2p)^5(3p)\}_l;J_l]+He+\Delta E_{k,l} \quad (1)$$

involving beams that are well characterized with respect to direction, velocity, and excited-state polarization. Strong, interesting polarization effects have been detected and absolute values of cross sections have been determined with a high accuracy of 25%.

Typical lifetimes of the $\{\alpha\}_k=\{(2p)^5(3p)\}_k$ states, with k running from 1 to 10 with decreasing energy, are $\tau=20$ ns. The total energy spread of the multiplet is $\Delta E_{1,10}=584$ meV. Although a large number, $\sum_{k=1}^{10}(J_k+1)=23$, of molecular states is involved, which complicates the analysis of the observed transitions, this system has two major advantages. First, the process of intramultiplet mixing has been investigated in detail in the afterglow of gas discharges, resulting in a suitable set of reference rate constants for Ne and He as collision partners.[11,16-18] Second, model potentials are available for the Ne**-He system, allowing a direct comparison of theory and experiment by means of full quantum-mechanical coupled-channels calculations.

A schematic view of the crossed-beam apparatus is given in Fig. 1. The short-lived $Ne^{**}(\{\alpha\}_k;J_k)$ atoms are produced by laser excitation of one of the metastable $Ne^*[\{(2p)^5(3s)\}]$ states. The primary beam of metastable atoms originates in a discharge-excited supersonic expansion. Downstream of the skimmer all charged particles are removed by condenser plates. A laser beam from a cw single-mode dye laser crosses the primary beam at a point 90 mm downstream of the source. This crossing point is located near the focus of

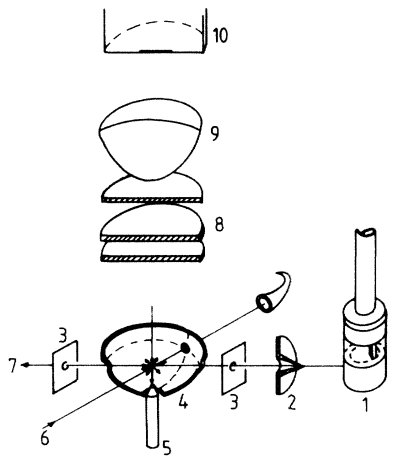

FIG. 1. Schematic view of the experimental setup. (1) primary-beam source; (2) skimmer; (3) beam collimators, 1 mm i.d.; (4) parabolic mirror; (5) secondary beam; (6) laser beam; (7) primary beam; (8) cutoff and interference filters; (9) lens; (10) photomultiplier in cooled housing.

a parabolic mirror. A skimmerless supersonic expansion, with a typical nozzle-to-primary beam distance $z_n = 2$ mm, provides a high-density secondary beam. The parabolic mirror focuses a large fraction (40% solid-angle efficiency) of the fluorescence radiation into a nearly parallel beam. Narrow-band interference filters (2 nm FWHM, 10 nm at 10^{-6} transmission) are used to select a single line of either the direct fluorescence from the initial state k or the collision-induced fluorescence from the final state l. These signals yield the number of atoms in the k and l states, respectively. Additional suppression of background light is achieved by the use of cutoff filters. The transmitted photons are focused on the 9-mm cathode of an S20 photomultiplier in a cooled housing. When we are measuring direct fluorescence radiation, gray filters are added to the optical system in order to guarantee a linear response of the photomultiplier.

The detection efficiency of the optical system is typically 10^{-3} per photon ($\lambda = 650$ nm) produced in the scattering volume. With primary- and secondary-beam densities of the order of $n_1 = 10^{13}$ m^{-3} and $n_2 = 5 \times 10^{20}$ m^{-3}, the overall figure of merit in the thermal energy range is about 2 kHz/Å^2 for the number of counts per unit of inelastic total cross section. The background counting rate ranges from 2 to 15 kHz and is mainly due to the line emission from the discharge in the primary-beam source.

In this Letter we report the polarization and energy dependence of the inelastic total cross section $Q_{7\leftarrow 5}$ for the collision-induced transition $\mathrm{Ne}^{**}(\{\alpha\}_5; J_5 = 1) \rightarrow \mathrm{Ne}^{**}(\{\alpha\}_7; J_7 = 1)$, with He as the collision partner. Using a linearly polarized laser beam and with the metastable $\mathrm{Ne}^*[\{(2p)^5(3s)\}; J = 0]$ state as lower level we excite the $|\{\alpha\}_5; Jm_J\rangle_{\mathbf{E}} = |\{\alpha\}_5; 1\,0\rangle_{\mathbf{E}}$ magnetic substate, with the electric field vector $\mathbf{E}$ as quantization axis at an angle β with the relative velocity vector $\mathbf{g}$. Scattering theory then predicts for the observed polarized cross section $Q^{\beta}_{7\leftarrow 5}(E)$

$$Q^{\beta}_{7\leftarrow 5}(E) = Q^{|0|}_{7\leftarrow 5}(E)\cos^2\beta + Q^{|1|}_{7\leftarrow 5}(E)\sin^2\beta, \tag{2}$$

with $Q^{|M_J|}_{7\leftarrow 5}(E)$ the polarized-emission cross section for a well defined initial asymptotic quantum number $|M_J|_{\mathbf{g}}$ with respect to the relative velocity, i.e., the asymptotic Ω value.

In Fig. 2 we show the experimental results $Q^{\beta}_{7\leftarrow 5}$ for the $\{\alpha\}_5 \rightarrow \{\alpha\}_7$ transition with $\Delta E_{5,7} = 80.7$ meV, at a center-of-center energy $E = 100$ meV. The measurements have been performed by variation of the angle θ between the primary-beam velocity $\mathbf{v}_1$ and $\mathbf{E}$, yielding extrema at angles $\theta = \theta_0$ and $\theta = \theta_0 + \pi/2$. By considering the Newton diagram of the collision process and taking into account that extrema occur at $\beta = 0$ and $\beta = \pi/2$, we can determine which of these extrema in θ corresponds to $\mathbf{E} \parallel \mathbf{g}$, i.e., $\theta = \theta_g$ and $\beta = 0$. From the orientation θ_g of the relative velocity vector in the laboratory system, the absolute value of the relative velocity and thus the collision energy may be readily calculated, with the well known values of the laboratory velocities $\mathbf{v}_1$ and $\mathbf{v}_2$ as input. Together with the nozzle-to-primary beam distance z_n, the angle $\theta = \theta_g$ also yields the effective position of the collision volume on the primary-beam axis. This information may then be used to determine the secondary-beam density and the acceptance of the optical system. At present we estimate the overall accuracy of the resulting absolute cross sections at 25%.

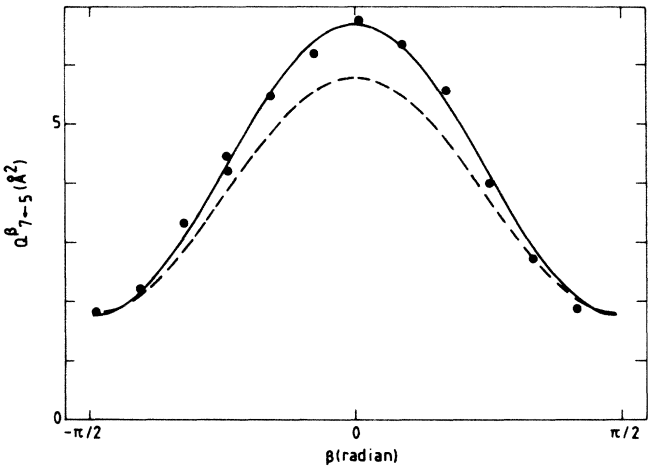

FIG. 2. Experimental results for the observed polarized-emission cross section $Q^{\beta}_{7\leftarrow 5}$ as a function of the angle β between the electric field $\mathbf{E}$ of the laser and the relative velocity $\mathbf{g}$, at a center-of-mass energy $E = 100$ meV. The statistical error is less than the size of the data points. The solid line is a curve fit according to Eq. (2). The dashed line is the prediction of the model potential of Hennecart and Masnou-Seeuws.

In Fig. 3 we show the observed energy dependence of the polarized-emission cross sections $Q^{|0|}_{7\leftarrow 5}$ and $Q^{|1|}_{7\leftarrow 5}$. The datum point at energy $E = 165$ meV has been obtained with a 90% He/10% Ne seeded primary beam. The He* metastable atoms are converted with approximately 50% efficiency into Ne* atoms by the He*-Ne excitation-transfer reactions. The other data points have been measured by variation of the position of the laser beam along the primary-beam axis, which results in different center-of-mass energies. We observe a good agreement between the two experimental methods. Errors in the energy are typically 5%, due both to the uncertainty and spread of the measured (Ne*) or calculated (He) velocity distributions of the colliding atoms, and to the uncertainty of the angle θ_g.

To obtain insight into the mechanisms underlying

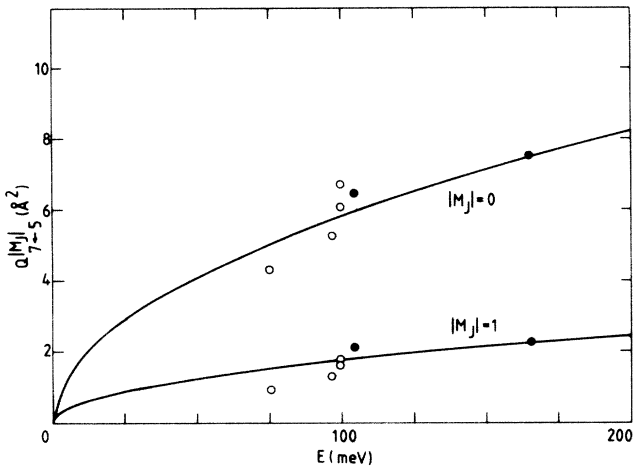

FIG. 3. Energy dependence of the polarized-emission cross sections $Q^{|0|}_{7\leftarrow 5}$ and $Q^{|1|}_{7\leftarrow 5}$, with E the center-of-mass energy. The full points have been obtained by varying the magnitude of the primary-beam velocity $\mathbf{v}_1$; the open points by varying the direction of $\mathbf{v}_2$ by scanning the laser beam along the primary-beam axis. The solid lines indicate the functional behavior $Q^{|M_J|}_{7\leftarrow 5} \sim E^{1/2}$.

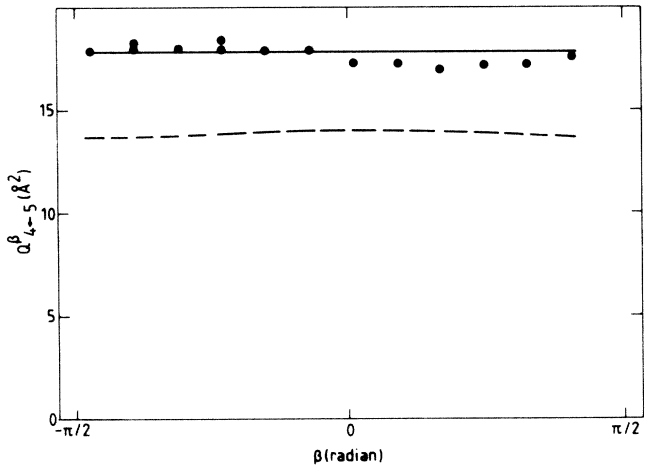

FIG. 4. Experimental results for the observed cross section $Q^{\beta}_{4\leftarrow 5}$ at $E = 100$ meV (the solid line indicates the average value), in comparison with the predictions of the model potentials of Hennecart and Masnou-Seeuws (dashed line). The data points have not been corrected for the nonisotropic distribution of collision-induced fluorescence radiation.

the surprisingly large polarization effects, we have to consider the salient features of the adiabatic potential curves involved, as calculated by Hennecart and Masnou-Seeuws[1,11] with a model potential method. We first discuss the $\{\alpha\}_5 \rightarrow \{\alpha\}_7$ transition. Both the initial and the final states show only a small splitting between the $\Omega = 0$ and $\Omega = 1$ molecular potentials. To indicate the range of internuclear distances R that is probed, at $E = 100$ meV the classical turning point for both Ω potentials of the $\{\alpha\}_5$ state is $R_t = 6a_0$ for an impact parameter $b = 0$ and $R_t = 7.1a_0$ for $b = 6a_0$. For $\Omega = 0$ the adiabatic electronic states are divided into 0^+ and 0^- classes, depending on the reflection symmetry. The $\Omega = 0^-$ class contains the $\{\alpha\}_{2,5,7,9,10}$ states and there is a strong coupling of the $\{\alpha\}_5$ and $\{\alpha\}_7$ states. This coupling can be identified as an avoided crossing at $R_c = 7.0a_0$ with a Landau-Zener-type coupling matrix element $H_{57} = 22$ meV (equal to half of the smallest separation of the potential curves), which is very large in comparison with the energy difference $\Delta E_{57} = 80.7$ meV of the $\{\alpha\}_5$ and $\{\alpha\}_7$ states at infinity. For $\Omega = 1$ there is no symmetry constraint and the intermediate $\{\alpha\}_6$ state disturbs the coupling of the $\{\alpha\}_5$ with the $\{\alpha\}_7$ state. We now observe an avoided crossing of the $\{\alpha\}_6$ and $\{\alpha\}_7$ states at $R_c = 7.5a_0$ with $H_{67} = 3.5$ meV. Moreover, the initial $\{\alpha\}_5$ state is now coupled to the $\{\alpha\}_4$ state by an avoided crossing with $H_{45} = 1.0$ meV at $R_c = 8.5a_0$. The small contribution of the $\Omega = 1$ orientation to the $\{\alpha\}_5 \rightarrow \{\alpha\}_7$ transition is due to the strong coupling of both the initial and final states to the $\{\alpha\}_4$ and $\{\alpha\}_6$ states, respectively, which is absent for the $\Omega = 0^-$ adiabatic potentials. The large coupling matrix element H_{57} for $\Omega = 0^-$ is consonant with a main contribution to the cross section from small impact parameters, where radial velocities are large. Even without "locking" of the initial $\Omega = |M_J|$ orientation to the internuclear axis, this orientation will then be largely conserved at the crossing radius. This results in the large polarization effect $Q^{|0|}_{7\leftarrow 5} >> Q^{|1|}_{7\leftarrow 5}$.

The picture that thus emerges is confirmed by the $\{\alpha\}_5 \rightarrow \{\alpha\}_4$ transition, for which the results are shown in Fig. 4. We note the absence of a significant polarization effect. This is in apparent contradiction with the simultaneous presence of an avoided crossing of the $\{\alpha\}_5$ and $\{\alpha\}_4$ states for the $\Omega = 1$ orientation, and the absence of any coupling at all for $\Omega = 0$ where initial and final states are in different symmetry classes. However, because of the small splitting of the $\{\alpha\}_5$ state between the $\Omega = 0$ and $\Omega = 1$ adiabatic potentials, the "locking" of the initial orientation to the internuclear axis constitutes only a minor effect. The asymptotic $|M_J| = 0$ orientation will thus be partially rotated at the crossing radius into a local $\Omega = 1$ state, which does couple with the final $\{\alpha\}_4$ state. This effect will be most pronounced for large impact parameters. Because of the very small coupling matrix element H_{45}, which requires small values of the radial velocity for optimum coupling, we indeed expect a predominant contribution from impact parameters $b \approx R_c$. Hence, the absence of a polarization effect, $Q^{|0|}_{4\leftarrow 5} \approx Q^{|1|}_{4\leftarrow 5}$, is qualitatively understood.

The total inelastic cross sections for the $\{\alpha\}_4 \rightarrow \{\alpha\}_5$ transition, as measured by Hennecart[11] in a

gas discharge, show a temperature dependence that is in agreement with a curve-crossing mechanism. This is supported by his calculation of the matrix elements of the radial coupling operator $\delta/\delta R$, which shows a localized coupling at $R = 8.5a_0$.

We have also performed a fully quantum-mechanical coupled-channels calculation using a diabatic basis $|\{\alpha\}_k; J_k \Omega \pi P M_P\rangle$, where the basis vectors have a well defined parity π, well defined quantum numbers P and M_P for the total angular momentum in the space-fixed frame, and well defined quantum numbers J and $\Omega = |M_J|_{z'}$ for the total electronic angular momentum in the body fixed frame, with z' along the internuclear axis. On this basis we have a maximum of 18 coupled equations for each value of P and $\pi = \pm 1$, because depending on parity the $\Omega = 0^-$ or 0^+ class is absent. We limit the calculation to P values corresponding to impact parameters $b \approx P\lambda\!\!\!^{-} \leq 15a_0$, with $\lambda\!\!\!^{-}$ the de Broglie wavelength in the incoming channel. For an energy $E = 100$ meV this comes down to $P \leq 100$.

The results of these calculations are given in Figs. 2 and 4. Because the model potentials of Hennecart and Masnou-Seeuws,[1,11] which have been used as input, are available only for $R \geq 4.5a_0$, a hard-sphere core has been added. However, this does not influence the results. We observe that theoretical predictions for both transitions are in fair agreement with the measurements.

In conclusion, we can state that the model potentials of Hennecart and Masnou-Seeuws provide a sufficient basis for both a simple qualitative description and a quantitative coupled-channels calculation.

The localized radial couplings in the $\{\alpha\}_{4,5,6,7}$ group and the absence of "locking" phenomena open up the prospect of a semiclassical description in terms of the Landau-Zener formalism for avoided crossings and a simple geometrical interpretation of rotational coupling. Future measurements of the energy dependence of all transitions in this group of four levels will have to show whether this is possible. The available center-of-mass energies are $0.1\ \text{eV} \leq E \leq 5$ eV, where a hollow-cathode arc[19] will be used for the high energy range.

[1]D. Hennecart and F. Masnou-Seeuws, J. Phys. B **18**, 657 (1985).

[2]W. Buszert, T. Bregel, R. J. Allan, M. W. Ruf, and H. Hotop, Z. Phys. A **320**, 105 (1985).

[3]M. H. Alexander, T. Orlikowski, and J. E. Straub, Phys. Rev. A **28**, 73 (1983).

[4]G. Nienhuis, Phys. Rev. A **26**, 3137 (1982).

[5]J. G. Kircz, R. Morgenstern, and G. Nienhuis, Phys. Rev. Lett. **48**, 610 (1982).

[6]H. A. J. Meyer, H. P. van der Meulen, and R. Morgenstern, to be published.

[7]D. Neuschäfer, M. O. Hale, I. V. Hertel, and S. R. Leone, to be published.

[8]M. O. Hale, I. V. Hertel, and S. R. Leone, Phys. Rev. Lett. **53**, 2296 (1984).

[9]M. O. Hale and S. R. Leone, Phys. Rev. A **31**, 103 (1985).

[10]A. Bahring, I. V. Hertel, E. Meyer, W. Meyer, N. Spies, and H. Schmidt, J. Phys. B **17**, 2859 (1984).

[11]D. Hennecart, J. Phys. (Paris) **39**, 1065 (1978), and thesis, Université de Caen, 1982 (unpublished).

[12]I. V. Hertel, Rep. Prog. Phys. **48**, 375 (1985).

[13]J. M. Mestdagh, J. Berlande, P. de Pujo, J. Cuvallier, and A. Binet, Z. Phys. A **304**, 3 (1982).

[14]E. Düren, E. Hasselbrink, and H. Tischen, Phys. Rev. Lett. **50**, 1983 (1983).

[15]L. Hüwel, J. Maier, and H. Pauly, J. Chem. Phys. **76**, 4961 (1982).

[16]M. J. Webster and M. J. Shaw, J. Phys. B **12**, 3521 (1979).

[17]F. C. M. Coolen, N. van Schaik, R. M. M. Smits, M. Prins, and L. W. G. Steenhuysen, Physica (Amsterdam) **93B+C**, 131 (1978); R. M. M. Smits, thesis, Eindhoven University of Technology, 1977 (unpublished).

[18]R. S. F. Chang and D. W. Setser, J. Chem. Phys. **72**, 4099 (1980).

[19]P. G. A. Theeuws, H. C. W. Beyerinck, D. C. Schram, and N. F. Verster, J. Phys. E **15**, 573 (1982).